

InterPACKICNMM2015-48317

FLOW BOILING HEAT TRANSFER COEFFICIENT OF DI-WATER/SIO₂ NANOFLUID INSIDE A 1.1 MM ROUND MICROCHANNEL

Tiago A. Moreira

Heat Transfer Research Group
University of Sao Paulo
Sao Carlos, SP, Brazil

Francisco J. do Nascimento

Heat Transfer Research Group
University of Sao Paulo
Sao Carlos, SP, Brazil

Gherhardt Ribatski

Heat Transfer Research Group
University of Sao Paulo
Sao Carlos, SP, Brazil

ABSTRACT

The scope of the present paper is the evaluation of the heat transfer coefficient during flow boiling of DI-water/silica nanofluid inside a 1.1 mm ID tube. The experiments were performed for nanoparticles and DI-water with both having thermal conductivities of the same order of magnitude ($k_{\text{DI-water}} = 0.6 \text{ W/mK}$, $k_{\text{silica}} = 1.4 \text{ W/mK}$). So, it was possible investigating the effect of the nanoparticles on the heat transfer coefficient under condition of negligible thermal conductivity enhancement. Experiments were carried out for mass velocities of 200, 400 and 600 kg/m²s, heat fluxes from 60 kW/m² to 350 kW/m² and nanoparticles volumetric concentration of 0.001%, 0.01% and 0.1%. Moreover, flow boiling heat transfer data under similar experimental conditions were obtained for DI-water without nanoparticles before and after performing each nanofluid test. The experiments were performed at the same test section according to the following sequence: i) DI-water, ii) 0.001% vol. nanofluid, iii) DI-water, iv) 0.01% vol. nanofluid, v) DI-water, vi) 0.1% vol. nanofluid, and vii) DI-water. Such procedure was adopted in order to evaluate the influence of the deposition of nanoparticles at each concentration on the heat transfer coefficient. For single-phase flow the HTC decreases as the experiments were performed. The thermal resistance due to deposition of nanoparticles is relevant to the heat transfer coefficient for single-phase flow of nanofluids inside microchannels. The flow boiling HTC decreases with increasing the nanoparticle volumetric concentration from a concentration of 0.001%. Based on the flow boiling HTC behaviors for tests with pure DI-water before and after the nanofluid tests, the fact that the HTC decreases with increasing

the nanoparticle volumetric concentration is not explained only by the deposition on the surface of a nanoparticle layer. Tests for pure DI-water before the tests of nanofluids (BBN condition) and after all the nanofluids tests (ABN 0.1% condition) presents similar heat transfer coefficients, despite the deposition of a nanoparticle layer on the surface.

INTRODUCTION

Great effort has been demanded to understand the complex mechanisms involved during heat transfer process of nanofluids since this denomination was proposed by Choi and Eastman (1995). In their study, nanoparticles were added to a fluid to enhance its thermal conductivity. Besides altering the transport properties of the base fluid, authors also identified that boiling of nanofluids leads to deposition of nanoparticles on the boiled surface, affecting the boiling mechanism. Controversial conclusions are found in the literature about the effect of using nanofluids on the heat transfer coefficient during boiling processes. On the other hand, it is fact that the critical heat flux increases with adding nanoparticles to a base fluid. Some literature reviews concerning experimental investigations of the boiling phenomena of nanofluids are listed below and are suggested to those interested on the state of the art concerning this topic: Eastman et al. (2004), Das et al. (2006), Cheng et al. (2008), Wang and Mujumdar (2008), Yu et al. (2008), Taylor and Phelan (2009), Wen et al. (2009), Godson et al. (2010), Barber et al. (2011), Cheng and Liu (2013), Taylor et al. (2013), Wu and Zhao (2013), Vafaei and Borca-Tasciuc (2014).

From an analyses of the literature reviews above mentioned, it is concluded that flow boiling of nanofluids

inside narrow channels was rarely investigated. Compared to results for the heat transfer coefficient during flow boiling of pure water, Wu et al. (2009) found increments up to 20% for convective boiling of alumina-water nanofluids. Boudouh et al. (2010) found increments of more than 100% in the heat transfer coefficient for flow boiling of copper-water nanofluids. Chegade et al. (2013), using silver-water nanofluids, found average increments for the flow boiling heat transfer coefficient up to 136% compared to pure water. Despite of the HTC enhancement pointed out by these studies, additional investigations are still needed in order to characterize the effect of nanofluids on the flow boiling mechanism inside microchannels.

In the present study, the heat transfer coefficient of DI-water/silica nanofluid inside a 1.1 mm ID tube is investigated for volumetric concentrations of nanoparticles (silica - SiO₂, 80 nm diameter) in water of 0.001, 0.01 and 0.1%, mass fluxes of 200, 400 and 600 kg/m²s and heat fluxes up to 350 kW/m².

EXPERIMENTAL TEST SETUP

The test facility consists of a closed loop and was validated based on comparisons of results for single-phase flow experiments for DI-water and well-established predictive methods. Figure 1 illustrates the experimental loop and details of the test section. In the apparatus, the test fluid is driven from the reservoir through the circuit by a gear pump (Micropump GA-T23). The mass flow rate is estimated from single-phase pressure drop measurements through a 2.0 mm ID quartz tube, 100 mm long using a differential pressure transducer (Endress+Hauser PMD75) with a measurement span of 0-3 kPa. Calibration curves were previously adjusted correlating the pressure drop and the volumetric flow rate, using as reference the rate of mass deposition in a digital analytical balance (precision of 0.01g) with the test facility operating as an open circuit. The mass flow rate is estimated from the volumetric flow rate based on the fluid density. Such procedure was implemented to avoid possible effects on the flow rate measurements of nanoparticles deposition on the internal parts of commercial and non-internally inspectable flow meters. The error associated with the mass flow rate was estimated as 4.6% of the measured value.

A pre-heater consisting of a tube-in-tube heat exchanger is used to impose the inlet temperature of the test fluid at the test section. This heat exchanger uses heating source water having its temperature controlled by a thermal bath. Needle valves located upstream and downstream of the test section are used to minimize two-phase flow oscillations due to compressible volumes. At the test section entrance, the bulk temperature (thermocouple within the flow) and absolute pressure (Endress+Hauser PMP131 for 0-400 kPa) are measured. The differential pressure along the test section (Endress+Hauser PMD75 for 0-300 kPa) and temperature of the exit flow are also measured. The wall temperature was measured with thermocouples fixed on the external wall of the test section at the top and bottom of each section. Wall temperatures were

measured at 5 cross-sections along the heated length (159.4mm) of the test tube. The test section is a stainless steel tube (AISI304) with internal diameter of 1.1 mm heated by Joule effect. Electrical current from a DC power source (TDK-Lambda GEN 20V-76A) was supplied directly to the test surface. All the temperatures were measured with K-type thermocouples. Just downstream the test section is a 1.0 mm ID quartz tube, 100 mm long, installed in order of allowing visualizations of the two-phase flow with a high-speed camera. Downstream the transparent tube is a heat exchanger (condenser) responsible for condensing and subcooling the test fluid by rejecting heat to a secondary fluid which temperature is controlled by a second thermal bath. The condenser, the pre-heater, the flow meter and the reservoir are made of borosilicate glass allowing the evaluation of the deposition of nanoparticles along the circuit. To record the data and to monitor and control de experimental apparatus, a LabView data acquisition system was used (SCXI-1000 with SCXI-1102 thermocouples module).

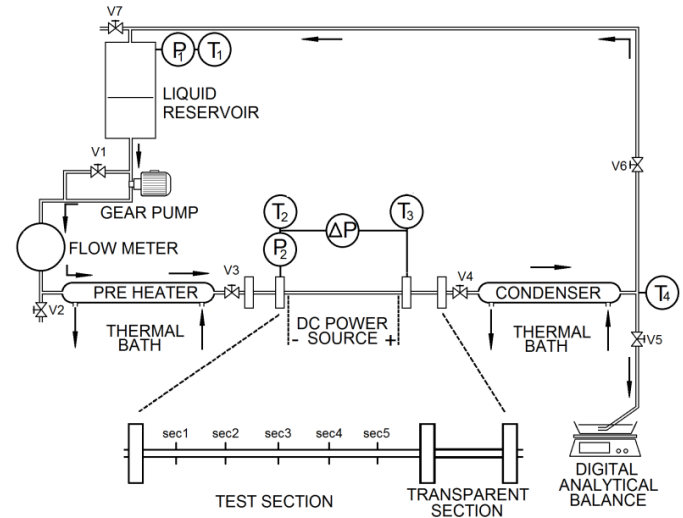


Figure 1 Illustration of the test facility and details of the test section. T represents the temperature measurement, P and ΔP the absolute and differential pressure measurement, respectively, and V the valves locations.

The nanofluids were prepared according to the two-steps method, which consists of adding nanoparticles, (silica - SiO₂ nanoparticles with 80 nm diameter) weighed through a digital analytical balance, to a base fluid (DI-water) and dispersing them through ultrasonication during a period of 30 minutes (Cole-Parmer CP505). Once prepared, the nanofluid was loaded into the test facility and experiments were performed as quickly as possible to minimize nanoparticles sedimentation.

TEST PROCEDURES

Heat transfer coefficient results were obtained using a single test section for the following conditions: (i) DI-water before

tests with nanofluids (BBN); (ii) 0.001% vol. concentration silica nanofluid; (iii) DI-water (ABN 0.001%); (iv) 0.01% vol. concentration silica nanofluid; (v) DI-water (ABN 0.01%); (vi) 0.1% vol. concentration silica nanofluid and (vii) DI-water (ABN 0.1%). The tests for each nanofluid were performed all at once and, then, the test fluid was removed at the end of the experiments, in order of avoiding the deposition and sedimentation of nanoparticles on the internal surfaces of the test circuit. After removing the nanofluid, the test facility was “cleaned” by repeating a procedure consisting on charging the circuit with DI-water and, then, circulating and draining the fluid. Before being charged in the circuit, the solution was boiled during a period of 30 minutes in order of eliminating non-condensable gases. The test circuit was firstly evacuated down to an absolute pressure of 10 kPa, and then charged with the test fluid.

The tests were performed for saturation temperature at the test section outlet of $102 \pm 3^\circ\text{C}$, subcooling at the test section inlet of 25°C , heat fluxes from 60 to 350 kW/m^2 , vapor quality at the test section outlet from 0.001 to 0.5 and mass velocities of 200, 400, 600 $\text{kg/m}^2\text{s}$. The local heat transfer coefficient, h , was estimated according to the Newton's cooling law, as follows:

$$h = \frac{q}{(T_{\text{wall}} - T_{\text{bulk}})} \quad (1)$$

The temperature at each of the five cross-sections of the heated length is estimated by averaging the values obtained from thermocouples placed on the top and bottom of the tube external surface. Based on this value, the wall temperature of the inner surface, T_{wall} , is estimated as follows:

$$T_{\text{wall}} = T_{\text{wall,ext}} + \frac{q}{2k_p} \left(\frac{(r_{\text{ext}}^2 - r_{\text{int}}^2)}{2} + r_{\text{ext}}^3 \ln\left(\frac{r_{\text{int}}}{r_{\text{ext}}}\right) \right) \quad (2)$$

This equation was deduced taking into account one-dimensional conduction through the wall, uniform heat generation by Joule effect and adiabatic external surface. To estimate the fluid bulk temperature, T_{bulk} , firstly, based on the heat flux and the measured temperature and pressure at the test section inlet, the subcooled region length, the single-phase pressure drop over its length, and the saturation temperature at the beginning of the saturated region were calculated by solving simultaneously an equation of state relating saturation temperature and pressure plus single-phase pressure drop and a local energy balance, given by:

$$i_i = \frac{Q}{m} + i_{i-1} \quad (3)$$

Where i_i is the local enthalpy and i_{i-1} is the enthalpy in the previous section of a discrete element in length of the test section. The overall pressure drop over the saturated region was then determined by subtracting the single-phase pressure drop from the measured total pressure drop. After that, a constant pressure drop gradient given by the ratio of the overall pressure

drop over the saturated region and its length was assumed from the beginning of the saturated region until the end of the test section. Then, the saturation temperature was calculated from the estimated local saturation pressure. The heat flux, q , was calculated as the ratio between the electrical power supplied to the test section and its internal area based on the heated length, where the electrical power was given by the product between the electrical current and voltage supplied by the DC power source. The vapor quality was determined by an energy balance over the heated length, as follows:

$$x = \frac{i - i_l}{i_v - i_l} \quad (4)$$

Temperature measurements were calibrated and the temperature uncertainty was evaluated according to the procedure suggested by Abernethy and Thompson (1973). Accounting for all instrument errors, uncertainties for the calculated parameter were estimated using the method of sequential perturbation according to Moffat (1988). The experimental heat transfer coefficient error was always smaller than 30%. The HTC average absolute error was 10.6%.

RESULTS

Figure 2 illustrates the variation of the heat transfer coefficient (HTC) along the test section under single-phase flow conditions and the theoretical HTC curve based on Churchill and Ozoe (1973). As result of flow development effects, the heat transfer coefficient decreases along the tube length and tends to a constant value at a distance from the tube inlet of approximately 0.1 m. It is also noted in Fig. 2 that the HTC decreases with increasing the nanoparticle volumetric concentration, even for the lowest nanoparticles concentration of 0.001% in volume.

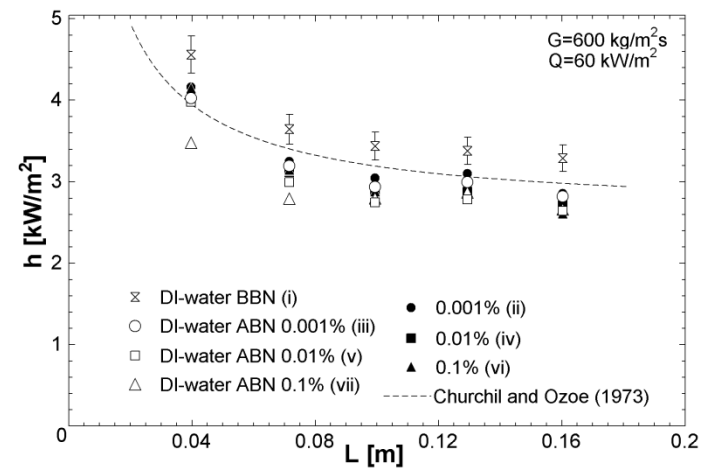


Figure 2: Single-phase heat transfer coefficient for $G=600 \text{ kg/m}^2\text{s}$ and $q=60 \text{ kW/m}^2$.

Moreover, lower HTC are displayed for the tests with DI-water ABN 0.1% at the two first sections where the wall temperature is measured. This result is explained by possible changes on the surface due to the deposition of nanoparticles during flow boiling of nanofluids. Figure 3 shows an image of the internal surface of the test section for the tube as received and after performing all the experiments at the first and fifth cross section containing thermocouples for wall temperature measurements. The images were obtained from axial cuts of the tube using a Nikon D5200 camera associated with a Nikon E200 microscope with magnification of four times. It can be noted from Fig. 3 that the deposition of nanoparticles is more intense close to the entrance of the test section and less intense close to the outlet.

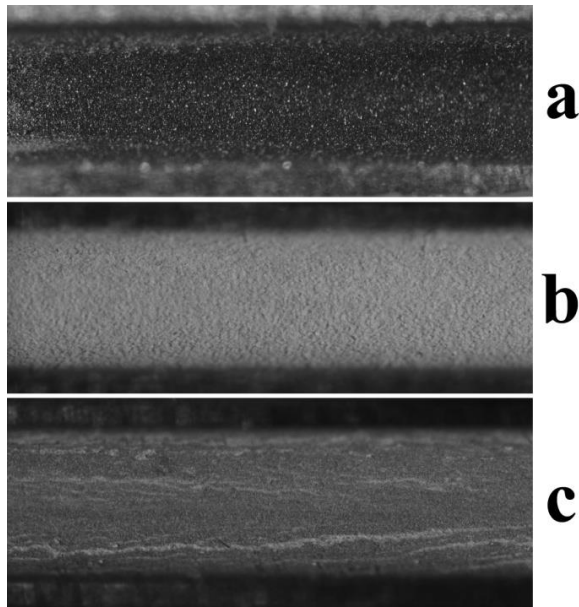


Figure 3: Images from axial cut of the test section (a) tube as received, (b) after all the silica nanofluids tests for the first thermocouple section and (c) the fifth thermocouple section.

According to the literature, variations of the transport properties due to the addition of nanoparticles to DI-water are indicated as responsible for variations in the heat transfer coefficient. So, in the present study the thermal conductivity (Hukseflux TP-08 probe), surface tension (SensaDyne QC6000) and viscosity (Brookfield DV-III Ultra - Cone/Plate CP40) of the nanofluids were evaluated at a temperature of $25.0 \pm 0.1^\circ\text{C}$. From these measurements, it was concluded that variations of the properties are only marginal and within the error band of the equipment. In a previous study (Moreira et al., 2015), the effect of adding alumina nanoparticles to DI-water was evaluated for the same experimental conditions, nanoparticles volumetric concentration and using the same test facility. In this study, a thermal conductivity augmentation of 44% relative to pure DI-water was found for a volumetric

concentration of alumina nanoparticles of 0.1%. This thermal conductivity enhancement affects positively the HTC for single-phase flow.

For a mass velocity of $600 \text{ kg/m}^2\text{s}$, heat flux of 60 kW/m^2 and under single-phase flow conditions, the pressure drop of DI-water (ABN) and DI-water (BBN) was considered to be the same once the difference of the values was within the error band of the differential pressure transducer. This result was already expected for single-phase flow because the effect of surface roughness under such condition is negligible and no effect on the viscosity is observed with the addition of nanoparticles to DI-water, as mentioned before.

Figures 4 to 6 illustrate flow boiling HTC results for DI-water and nanofluids. For each mass velocity, similar conclusions can be drawn for different heat fluxes.

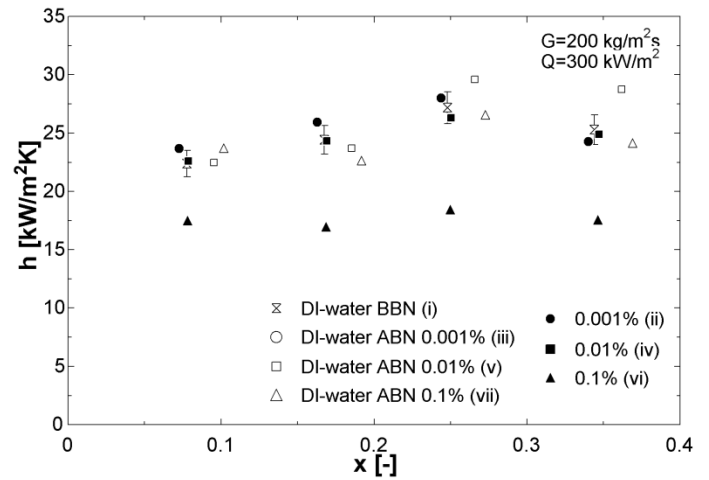


Figure 4: Two-phase HTC for $G=200 \text{ kg/m}^2\text{s}$ and $q=300 \text{ kW/m}^2$.

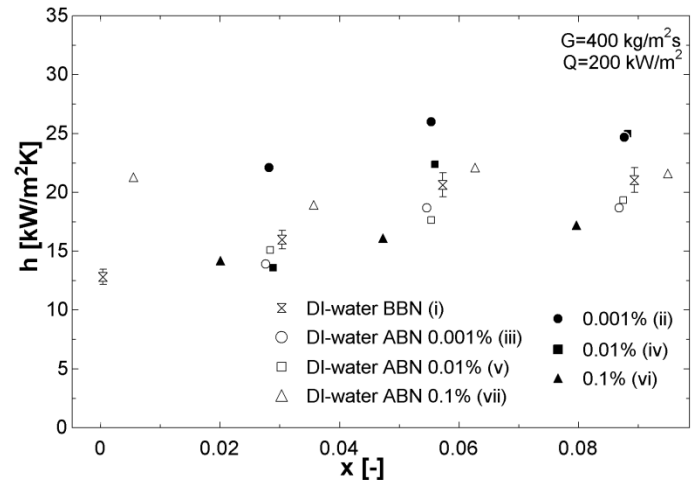


Figure 5: Two-phase HTC for $G=400 \text{ kg/m}^2\text{s}$ and $q=200 \text{ kW/m}^2$.

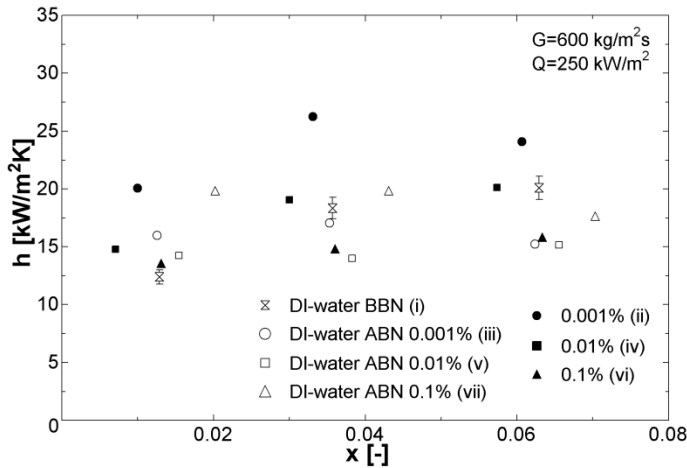


Figure 6: Two-phase HTC for $G=600\text{kg/m}^2\text{s}$ and $q=250\text{ kW/m}^2$.

It can be noted in Figs. 4 to 6 that the lowest nanoparticle concentration in DI-water provides the highest flow boiling HTC. This behavior becomes more evident as the mass flux increases. The lowest two-phase HTC is observed for the highest nanoparticles concentration (0.1% vol.). It is also noted in Figs. 4 to 6 that the HTC for DI-water BBN and DI-water ABN for a concentration of 0.1% are not significantly different opposite to what was observed by Moreira et al. (2015) for alumina nanoparticles in DI-water. Another conclusion from the experimental data is that for flow boiling of DI-water/silica nanofluids the HTC decreases with increasing nanoparticles concentration from a volumetric concentration of 0.001%. The effect of nanoparticle concentration is not evident for the tests with pure DI-water before and after the tests with nanofluids. This result suggests that only the deposition of a nanoparticle layer, promoting an additional thermal resistance, does not explain the reduction of the flow boiling HTC from a concentration of 0.001%.

Moreira et al. (2015) observed that the flow boiling instabilities due to the boiling process under confined condition decreases significantly with the addition of alumina nanoparticles to the DI-water even for the lowest nanoparticles concentration (0.001% vol.). In the present study, the effect of the nanoparticles addition to DI-water on the flow boiling instabilities characterized by temperature, pressure fluctuations and back-flows was not evident.

CONCLUSIONS

Single-phase flow HTC data of nanofluids composed of DI-water+SiO₂) were gathered and their analyses revealed that the thermal resistance due to deposition of nanoparticles is relevant to the heat transfer coefficient for single-phase flow of nanofluids inside microchannels.

The flow boiling heat transfer coefficient of the nanofluid (DI-water+SiO₂) with a volumetric concentration of 0.001% was higher than the HTC of pure DI-water before the tests with

nanofluids (BBN condition). The flow boiling HTC decreases with increasing the nanoparticle volumetric concentration from a concentration of 0.001%. Based on the flow boiling HTC behaviors for tests with pure DI-water before and after the nanofluid tests, the fact that the HTC decreases with increasing the nanoparticle volumetric concentration is not explained only by the deposition on the surface of a nanoparticle layer. Tests for pure DI-water before the tests of nanofluids (BBN condition) and after all the nanofluids tests (ABN 0.1% condition) presents similar heat transfer coefficients, despite the deposition of a nanoparticle layer on the surface. The nanoparticle deposition was more intense at the initial length of the heated surface. The effect on the thermal instabilities of adding silica nanoparticles to DI-water was negligible.

NOMENCLATURE

ABN	After boiling of nanofluids
BBN	Before boiling of nanofluids
ΔP	Differential pressure drop, kPa
G	Mass velocity, $\text{kg/m}^2\text{s}$
h	Heat transfer coefficient, $\text{kW/m}^2\text{K}$
i	Enthalpy, kJ/kgK
i_l	Saturated liquid enthalpy, kJ/kgK
i_v	Saturated enthalpy, kJ/kgK
k_p	Thermal conductivity of the tube; W/mK
L	Test section length, m
ID	Internal diameter
m	Mass flow; kg/s
P	Pressure, kPa
q	Heat flux, kW/m^2
Q	Power applied, kW
r_{int}	Internal radius, m
r_{ext}	External radius, m
Sec	Temperature cross section
T	Temperature, °C
V	Valve
x	Vapor quality
z	Tube position from the inlet, m

ACKNOWLEDGMENTS

The authors gratefully acknowledge the financial support under contract numbers 2011/13119-0 and 2013/02869-4 given by FAPESP (Sao Paulo Research Foundation, Brazil) and the research grant given by CAPES (Coordination for the Improvement of Higher Level Personnel, Brazil) through the NANOBIOTEC research program. The grant under contract number 303852/2013-5 given by CNPq (National Council of Technological and Scientific Development, Brazil) is also acknowledged. The technical support given by Mr. José Roberto Bogni is appreciated and recognized.

REFERENCES

- Abernethy R.B., Thompson J.W., 1973. Handbook uncertainty in gas turbine measurements, *Arnold Engineering Development Center, Arnold Air Force Station, Tennessee*.

- Barber, J., Brutin, D., Tadrist, L., 2011.** A review on boiling heat transfer enhancement with nanofluids, *Nanoscale Res. Lett.*, Vol. 6, pp. 1-16.
- Boudouh, M., Gualous, H.L., De Labachellerie, M., 2010.** Local convective boiling heat transfer and pressure drop of nanofluid in narrow rectangular channels, *Appl. Therm. Eng.*, Vol. 30, pp. 2619–2631.
- Cehade, A.A., Gualous, H.L., Le Masson, S., Fardoun, F., Besq, A., 2013.** Boiling local heat transfer enhancement in minichannels using nanofluids, *Nanoscale Res. Lett.*, Vol. 8, pp. 1-20.
- Cheng, L., Bandarra Filho, E.P., Thome, J.R., 2008.** Nanofluid Two-Phase Flow and Thermal Physics: A New Research Frontier of Nanotechnology and Its Challenges, *J. Nanosci. Nanotechnol.*, Vol. 8, pp. 3315–3332.
- Cheng, L., Liu, L., 2013.** Boiling and two-phase flow phenomena of refrigerant-based nanofluids: Fundamentals, applications and challenges, *Int. J. Refrig.*, Vol.36, pp. 421–446.
- Choi, S.U.S., Eastman, J.A., 1995.** Enhancing Thermal Conductivity of Fluids with Nanoparticles, in: *ASME International Mechanical Engineering Congress & Exposition*. San Francisco, CA, USA.
- Churchill, S.W., Ozoe, H., 1973.** Correlations for Laminar Forced Convection with Uniform Heating in Flow over a Plate and in Developing and Fully Developed Flow in a tube, *J. of Heat Transfer*, Vol. 95, pp. 78-84.
- Das, S.K., Choi, S.U.S., Patel, H.E., 2006.** Heat Transfer in Nanofluids—A Review, *Heat Transf. Eng.*, Vol.27, pp. 3–19.
- Eastman, J. a., Phillpot, S.R., Choi, S.U.S., Keblinski, P., 2004.** Thermal Transport in Nanofluids, *Annu. Rev. Mater. Res.*, Vol. 34, pp. 219–246.
- Godson, L., Raja, B., Mohan Lal, D., Wongwises, S., 2010.** Enhancement of heat transfer using nanofluids—An overview, *Renew. Sustain. Energy Rev.*, Vol.14, pp. 629–641.
- Moffat, R.J., 1988.** Describing the Uncertainties in Experimental Results, *Exp. Thermal Fluid Science*, Vol. 1, pp. 3-17.
- Moreira, T. A., do Nascimento, F.J., Ribatski, G., 2015.** Flow boiling of nanofluids of water and Al₂O₃ inside a 1.1 mm round channel, *9th Int. Conf. on Boiling and Condensation Heat Transfer*, Boulder, CO, USA.
- Taylor, R., Coulombe, S., Otanicar, T., Phelan, P., Gunawan, A., Lv, W., Rosengarten, G., Prasher, R., Tyagi, H., 2013.** Small particles, big impacts: A review of the diverse applications of nanofluids, *J. Appl. Phys.*, Vol. 113, pp. 1-19.
- Taylor, R.A., Phelan, P.E., 2009.** Pool boiling of nanofluids : Comprehensive review of existing data and limited new data, *Int. J. Heat Mass Transf.*, Vol. 52, pp. 5339–5347.
- Vafaei, S., Borca-Tasciuc, T., 2014.** Role of nanoparticles on nanofluid boiling phenomenon: Nanoparticle deposition, *Chem. Eng. Res. Des.*, Vol. 92, pp.842–856.
- Wang, X., Mujumdar, A.S., 2008.** A review on nanofluids - Part II: Experiments and applications, *Brazilian J. Chem. Eng.*, Vol.25, pp. 631–648.
- Wen, D., Lin, G., Vafaei, S., Zhang, K., 2009.** Review of nanofluids for heat transfer applications, *Particuology*, Vol. 7, pp. 141–150.
- Wu, J.M., Zhao, J., 2013.** A review of nanofluid heat transfer and critical heat flux enhancement—Research gap to engineering application, *Prog. Nucl. Energy*, Vol. 66, pp. 13–24.
- Wu, X., Wu, H., Cheng, P., 2009.** Pressure drop and heat transfer of Al₂O₃ -H₂O nanofluids through silicon microchannels, *J. Micromechanics Microengineering*, Vol. 19, pp. 1-11.
- Yu, W., France, D.M., Routbort, J.L., Choi, S.U.S., 2008.** Review and Comparison of Nanofluid Thermal Conductivity and Heat Transfer Enhancements, *Heat Transf. Eng.*, Vol. 29, pp. 432–460.